INSTITUTE OF PHYSICS PUBLISHING JOURNAL OF PHYSICS B: ATOMIC, MOLECULAR AND OPTICAL PHYSICS

J. Phys. B: At. Mol. Opt. Phys. **35** (2002) 3157–3165 PII: S0953-4075(02)33056-6

Cusp formation in classical trajectory Monte Carlo calculations of ion-impact ionization collisions

R O Barrachina[1,3] **and C Courbin**[2]

[1] Centro Atómico Bariloche and Instituto Balseiro[4], 8400 S C de Bariloche, Río Negro, Argentina
[2] Laboratoire de Dynamique des Ions, Atomes et Molecules, Université P et M Curie,
4 Place Jussieu, T12-B75, F-75 252 Paris Cedex 05, France

Received 25 January 2002, in final form 7 June 2002
Published 10 July 2002
Online at stacks.iop.org/JPhysB/35/3157

Abstract

We study the formation of cusps in the double differential cross section for ion–atom ionization collisions by means of a classical trajectory Monte Carlo calculation. The use of an 'importance sampling' algorithm allows us to improve the efficiency of the method. We show that the overall shape of the cusp is decided during the collision stage, while its divergence builds up asymptotically as the result of a two-body process, in complete accordance with the general framework of the final state interaction theory.

1. Introduction

Our purpose in this paper is to elucidate, through numerical Monte Carlo simulations with classical trajectories, some of the qualitative and quantitative aspects of cusp formation in ion–atom ionization collisions. To focus the present discussion, we display in figure 1 the velocity spectrum $\mathrm{d}\sigma/\mathrm{d}\boldsymbol{v}$ of the electrons emitted from H(1s) targets by the collision of 100 keV H^+ projectiles. This spectrum is calculated by means of a classical trajectory Monte Carlo (CTMC) algorithm, as explained in the following sections. Two characteristic cusp-shaped peaks are clearly observed surrounding $\boldsymbol{v} = 0$ and $\boldsymbol{v}_\mathrm{P}$, where $\boldsymbol{v}_\mathrm{P}$ is the projectile velocity. The latter cusp is the so-called 'electron capture to the continuum' (or ECC) peak. It was experimentally discovered by Crooks and Rudd (1970) and theoretically explained by Macek (1970) more than three decades ago. This cusp was immediately visualized as the result of a smooth continuation across the ionization limit of *capture* into highly excited electron–projectile bound states (Rudd and Macek 1972). In this sense, the characteristic $1/|\boldsymbol{v} - \boldsymbol{v}_\mathrm{P}|$ divergence of the electron velocity distribution was ascribed to the fact that the corresponding discrete spectrum for the electron–projectile system accumulates at zero energy. Thus, it is no wonder that any classical description, by mimicking this bound spectrum by a continuum, would succeed in describing the ECC divergence. In 1989 Reinhold and Olson explicitly showed that a CTMC

[3] Also member of the Consejo Nacional de Investigaciones Científicas y Técnicas, Argentina.
[4] Comisión Nacional de Energía Atómica and Universidad Nacional de Cuyo, Argentina.

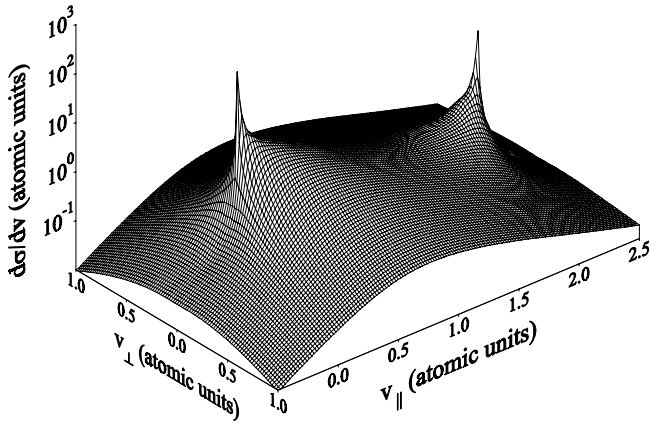

Figure 1. CTMC calculation of the differential cross section $d\sigma/dv$ for the ionization of H(1s) targets by the collision of 100 keV H^+ projectiles. The details of the algorithm are explained in the text. $v_\parallel$ and $v_\perp$ are the components of the electron velocity $\boldsymbol{v}$ parallel and perpendicular to the projectile velocity $\boldsymbol{v}_P$, respectively.

calculation does reproduce this cusp-shaped structure. However, it is important to point out that this success should not be mistakenly taken as a demonstration of a supposedly classical origin of this phenomenon. The classical description certainly works whenever the electron–projectile interaction is of a Coulomb type (Ovchinnikov and Khrebtukov 1987, Schultz *et al* 1996) or even of a dipolar nature (Tökési *et al* 1997, Sarkadi *et al* 2000). But, whenever the electron–projectile interaction decreases faster than a dipole potential at large distances, i.e. $r'^2\, V_{Pe}(r') \to 0$, the energy spectrum does not accumulate at zero energy, and the cusp displays a Lorentzian behaviour (Barrachina 1990, 1997) that cannot be reproduced by any classical description (Fiol *et al* 2002). This is the case, for instance, for a neutral polarizable projectile. The ECC cusp observed in coincidence with neutral He outcoming projectiles, first measured by Köver *et al* in 1989, is an example of this situation (see also Báder *et al* (1997)). These different behaviours provide additional evidence of the fact that cusp formation is essentially a two-body process, as it was understood many years ago. However, some recent works seem to suggest otherwise (e.g. Illescas *et al* (2002)). One of our goals is to demonstrate the two-body nature of the cusp in great detail, employing the same theoretical tools used in those works.

If the role of the projectile and the residual target ion is switched, these same ideas apply for the other $1/v$ diverging cusp observed at $\boldsymbol{v} = 0$ in figure 1. The momentum transferred from the projectiles to these so-called 'soft-collision electrons' is just enough to unbind them. If the parallelism with the ECC cusp is maintained, it is possible to call them 'electrons excited to the continuum' (EEC), and we shall keep this name, even though the 'soft-electron' (SE) denomination has prevailed in the literature.

2. The classical trajectory Monte Carlo method

The CTMC method has been applied with great success for the description of intermediate energy atomic collisions by different authors (Abrines and Percival 1966, Olson and Salop 1977, Bandarage and Parson 1990, Illescas *et al* 1998). In particular, it has been shown to be an invaluable and very versatile tool for the study of ionization collisions. For the purpose of this paper, it will suffice to analyse the simplest ion–atom collision, i.e. a typical $H^+ + H(1s) \to H^+ + H^+ + e^-$ single ionization process. The calculation procedure is described

in detail in a previous work (Fiol *et al* 2000), except that here we employ a somewhat different impact parameter statistic, as explained below.

A flux of H^+ ions of velocity $\boldsymbol{v}_P$ impinges from infinity upon a target consisting of H(1s) atoms. The initial conditions to describe the 1s electron orbiting around the nucleus are the energy of the Kepler orbit (−0.5 au), its eccentricity, the three Euler angles fixing the orbital plane and orientation in space, and the eccentric angle that defines the initial position of the electron along this orbit. After N calculated trajectories, the ionization cross section differential in the electron velocity $\boldsymbol{v}$ is approximated by the estimator

$$\frac{\mathrm{d}\sigma}{\mathrm{d}\boldsymbol{v}} = 2\pi \sum_b b \frac{\delta N_\mathrm{i}(b)}{\delta \boldsymbol{v}} \left(\frac{\mathrm{d}N}{\mathrm{d}b}\right)^{-1}, \tag{1}$$

where δN_i is the number of occasions on which the energy criterion for ionization is fulfilled and $\boldsymbol{v}$ ends within the range $\delta \boldsymbol{v}$. The distribution $\mathrm{d}N/\mathrm{d}b$ of impact parameters in the incoming beam verifies that

$$\int_0^\infty \frac{\mathrm{d}N}{\mathrm{d}b}\mathrm{d}b = N.$$

Usually, an incoming flux uniform in b^2 up to an arbitrary maximum impact parameter b_o has been used in the literature with near exclusivity. In this case

$$\frac{\mathrm{d}N}{\mathrm{d}b} = 2N\frac{b}{b_o^2}\Theta(b_o - b), \tag{2}$$

where $\Theta(x)$ is the Heaviside step function, and (1) reduces to the standard formula

$$\frac{\mathrm{d}\sigma}{\mathrm{d}\boldsymbol{v}} = \pi b_o^2 \sum_{b \leqslant b_o} \frac{1}{N} \frac{\delta N_\mathrm{i}(b)}{\delta \boldsymbol{v}}.$$

In the usual jargon of the Monte Carlo technique, this choice of $\mathrm{d}N/\mathrm{d}b$ reduces CTMC to what is known as a 'hit-or-miss' method (Hammersley and Handscomb 1964, Rubinstein 1981). This is reputed to be the most inefficient Monte Carlo algorithm, whatever calculations it is applied to (Hammersley and Handscomb 1964). In the case of CTMC, the arbitrariness in the choice of b_o and the dominance of large impact parameters, which are not prone to ionization collisions, are two symptoms of this inefficiency. Some authors (see, for instance, Lewartowski and Courbin (1992)) have employed a linear distribution

$$\frac{\mathrm{d}N}{\mathrm{d}b} = \frac{N}{b_o}\Theta(b_o - b), \tag{3}$$

which leads to a weighted estimator

$$\frac{\mathrm{d}\sigma}{\mathrm{d}\boldsymbol{v}} = 2\pi b_o \sum_{b \leqslant b_o} \frac{b}{N} \frac{\delta N_\mathrm{i}(b)}{\delta \boldsymbol{v}}.$$

This choice of $\mathrm{d}N/\mathrm{d}b$ is more efficient than the crude 'hit-or-miss' algorithm, but still maintains the arbitrariness of b_o and a slightly moderated dominance of large impact parameters.

In contrast, in this paper we employ an 'importance sampling' method over the impact parameter that is free of these two shortcomings. We start by choosing a distribution $\mathrm{d}N/\mathrm{d}b$ with a shape similar to that obtained by means of a first crude simulation. Then, this refined distribution is used to improve the efficiency of a second definitive simulation. This is shown in figure 2, where the quadratic (2) and linear (3) distributions (with an arbitrary choice of $b_o = 4$ au) are compared with a sampling optimized for the calculation of total ionization cross sections in 100 keV H^+ + H(1s) collisions. Note that this simple variance reduction technique favours the dominance of small impact parameters, leading to a dramatic increase

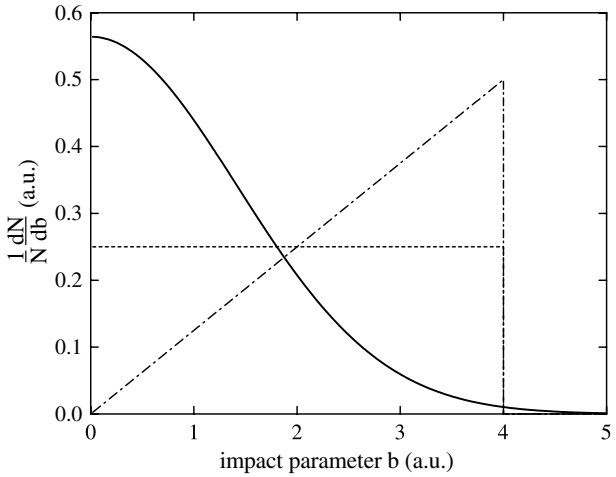

Figure 2. The quadratic (2) (chain curve) and linear (3) (broken curve) distributions of impact parameters (with an arbitrary choice of $b_o = 4$ au) usually employed in CTMC calculations are compared with an 'importance sampling' (full curve) optimized for the calculation of total ionization cross sections in 100 keV $H^+ + H(1s)$ collisions.

in the efficiency of the calculation. For the ionization of hydrogen targets by the impact of protons with a velocity of $v = 2$ au, the efficiency of the impact parameter distribution depicted in figure 2 is more than three times larger than the 'hit-or-miss' algorithm with a quadratic distribution (2). Redefining the sampling for each particular calculation, the efficiency can be improved even further. In particular, we evaluate the estimator for $d\sigma/dv$ by means of about 12×10^6 trajectories, but with a distribution optimized to achieve an efficiency equivalent to a homogeneous plane (quadratic) distribution of 50×10^6 trajectories with $b_o = 4$ au.

3. Classical description of cusp production

In their 1989 work, Reinhold and Olson explained the formation of the ECC cusp in CTMC calculations in terms of the dominance of two mechanisms. The most important one was the focusing of the electrons in the forward direction due to their interaction with the projectile in the asymptotic regime. In this sense, they pointed out that, in order to decide the final ejection angle of the ECC electrons, the integration of the canonical Hamilton equations has to be continued during an extremely long time. Secondly, they also proposed another mechanism where a fraction of the electrons that are captured to highly excited states may still be ionized at large internuclear distances by the residual target nucleus. Furthermore, this integration had to be carried out with high numerical precision so as not to ionize the electrons captured to highly excited orbits due to numerical error. As an aftermath of this perception of the main mechanisms for the ECC effect, different authors (see, for instance, Tökesi *et al* (1997), Sarkadi *et al* (2000) and Illescas *et al* (2002)) have assumed that the formation of a cusp in atomic collisions proceeds so slowly that, when it is evaluated by means of a CTMC calculation, it is necessary to integrate the Hamilton equations up to very large internuclear distances of the order of $R \approx 10^5$ au or even larger.

Figure 3 depicts the origin of this idea in a plot similar to that employed by Reinhold and Olson in 1989. Here we show the velocity distribution of the electrons that are detected in a direction parallel to that of the projectile motion for a $H^+ + H$ ionization collision at an impact

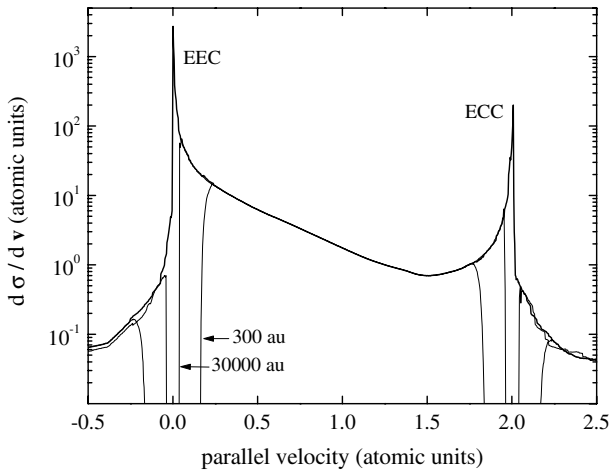

Figure 3. CTMC calculation of the differential cross section $d\sigma/dv$ for a $H^+ + H$ ionization collision at an impact energy of 100 keV. The velocity distribution of the emitted electrons is depicted in a direction parallel to that of the projectile's motion, when the integration of the Hamilton equations is stopped at two different internuclear distances $R = 300$ and 30 000 au. Also the same 0° cut of $d\sigma/dv$ is shown for the limit $R \to \infty$. The details of these calculations are explained in the text.

velocity of 2 au, when the integration of the Hamilton equations is stopped at two different internuclear distances $R = 300$ and 30 000 au. This same calculation was also performed keeping the interactions between the three particles 'alive' up to other internuclear distances of 100, 300, 1000, 3000, 10 000, 30 000 and 100 000 au. In order to have a clearcut representation of both cusps, we have employed a resolution volume δv that goes to zero not only for $v \to 0$, as in a typical collision experiment (Meckbach *et al* 1981), but also for $v' \to 0$, with $v' = v - v_P$. This condition is very severe on the CTMC algorithm, requiring a large amount of trajectories to get reasonable statistics, but at the same time yields a similar and quantitatively comparable description of both cusps. In particular, we used $\lim_{v\to 0} \delta v/v^3 = \lim_{v'\to 0} \delta v'/v'^3 = \mathcal{R}$ with $\mathcal{R}$ of the order of 5×10^{-4} au.

As expected from Reinhold and Olson's discussion, figure 3 clearly shows that no EEC or ECC peaks are obtained if the integration is stopped at any intermediate internuclear distance. The use of a good resolution and an electron emission exactly set to the forward and backward directions show that this lack of cusp structures pervades even at internuclear distances as large as $R = 3 \times 10^4$ au. It is not shown in the figure, but similar 'holes' at the positions of the EEC and ECC peaks, with a diameter of the order of 0.05 au, are still visible for $R = 10^5$ au. As the integration proceeds, these holes around $v = 0$ and v_P are filled up and the EEC and ECC cusps are slowly formed.

In a quantum mechanical description of cusp formation, each peak is solely produced by an enhancement factor given by the inverse square modulus of a two-body s-wave Jost function (Barrachina 1997, Fiol *et al* 2001b). For the ECC process, for instance, this Jost function relates the electron and the projectile alone. Thus, cusp formation is in essence a two-body (i.e. single-centre) process, where the third particle is a mere spectator that at most can affect its overall shape, but not its characteristic divergence. Being so, the projection of the electron trajectory onto one-centre orbits would suffice to recover the cusp divergency in a CTMC calculation (Schultz *et al* 1996). For instance, Reinhold *et al* (1992) employed this extrapolation technique for the simulation of cusp electron emission in ion–solid collisions, where the electron was

assumed to evolve in the Coulomb field of the projectile alone after exiting the solid surface. Furthermore, Tökesi *et al* (1994) justified its application for the study of the electron loss to the continuum (ELC) cusp in H + H collisions in view that the dipole-type electron–target interaction can be neglected at large distances. However, even nowadays authors using CTMC to calculate the ECC cusps in ion–atom collisions let the program proceed up to an internuclear distance R of the order of 10^5 au or larger. The associated computing effort involved in the use of such large values of R can only be explained if some relevant process is assumed to be taking place in the asymptotic region in the case of long-range Coulomb interactions. For instance, it has been asserted that even at these large distances the target–electron interaction plays an essential role in the asymmetry of the cusp (Illescas *et al* 2002). Let us investigate these ideas more carefully.

Let us first assume that, at a given time after the collision, the target is so far away from the emitted electron contributing to the ECC cusp that its influence is of no significance. We consider an electron moving at a distance $\boldsymbol{r}'$ from the projectile with relative velocity $\boldsymbol{v}' = \boldsymbol{v} - \boldsymbol{v}_{\mathrm{P}}$. Whenever its relative kinetic energy $mv'^2/2$ is smaller than the corresponding potential energy $-1/r'$ at a given time after the collision, it cannot escape from the projectile's attraction. This means that most of the electrons with small relative velocity $\boldsymbol{v}'$ are prone to remain captured. Thus, instead of a cusp, a hole with a clearcut edge at a given relative velocity v'_{h} is observed, as shown in figure 3. The sharpness of this edge implies that most of the electrons that satisfy the threshold condition $mv'^2/2 = 1/r'$ have velocities near v'_{h} (and are at a distance $r' \approx 2/mv'^2_{\mathrm{h}}$ from the projectile), as is assumed in the 'free expansion' model of Illescas *et al* (Illescas and Riera 1998, Illescas *et al* 2002). Those electrons with relative velocities larger than v'_{h} (i.e. outside the 'hole') have enough kinetic energy to escape from the projectile's attraction and build up the ECC cusp with a final relative velocity approximately equal to $v'_{\infty} \approx v'(1-2/mv'^2r')^{1/2}$. Meanwhile, the electrons inside the 'hole' remain attached to the projectile in a closed orbit and are never observed at asymptotic large distances. The edge of this ECC hole has the same origin as the constant value of the recoil ion momentum distribution at the kinematical threshold (Fiol *et al* 2000). The only difference is that, as the integration proceeds, this threshold remains fixed, while v'_{h} in the electron velocity distribution tends to zero and the $1/v'$ divergence is slowly formed. Thus, the ECC electrons are already there at a finite time after the collision, but not at a relative electron–projectile velocity equal to zero (since those electrons have not enough energy to escape from the Coulomb projectile attraction). In fact, the electrons near the edge of the hole will reach infinity with an asymptotic velocity of the order of $v'_{\infty} = \sqrt{v'^2 - 2/mr'} \approx \sqrt{v'^2 - v'^2_{\mathrm{h}}}$, and the final velocity distribution would read

$$\frac{\mathrm{d}\sigma}{\mathrm{d}\boldsymbol{v}'_{\infty}} = \frac{v'}{v'_{\infty}} \frac{\mathrm{d}\sigma}{\mathrm{d}\boldsymbol{v}'}.$$

We clearly see that the presence of a finite value of $\mathrm{d}\sigma/\mathrm{d}\boldsymbol{v}'$ at $v' = v'_{\mathrm{h}}$ means that $\mathrm{d}\sigma/\mathrm{d}\boldsymbol{v}'_{\infty}$ diverges like $1/v'_{\infty}$, i.e. the ECC cusp is recovered.

Let us analyse this transformation in more detail for the case of the EEC cusp. The calculations for the ECC peak proceed similarly, except for a simple Galilean transformation (see, for instance, Tökési *et al* (1994)). For given values of the position $\boldsymbol{r}$ and velocity $\boldsymbol{v}$ of the electron relative to the target nucleus, it is possible to get the final relative velocity $\boldsymbol{v}_{\infty}$ assuming that the electron–target system evolves independently from the projectile, which keeps an approximately constant velocity.

By conservation of energy, the modulus of the asymptotic velocity reads

$$v_\infty = v\sqrt{1 - \frac{1/r}{mv^2/2}}.$$

By conservation of angular momentum, $\boldsymbol{v}_\infty$ remains in the plane defined by $\boldsymbol{r}$ and $\boldsymbol{v}$, with axis

$$\hat{\boldsymbol{x}} = \boldsymbol{r}/r$$
$$\hat{\boldsymbol{y}} = (\boldsymbol{v} - v\hat{\boldsymbol{x}}\cos\alpha)/v\sin\alpha$$

and forms an angle θ with $\boldsymbol{r}$ that is given by (Samengo and Barrachina 1994)

$$\cos\theta = -1 + \frac{2(v\cos\alpha - v_\infty)^2}{v^2 + v_\infty^2 - 2vv_\infty\cos\alpha}$$

where α is the angle between $\boldsymbol{r}$ and $\boldsymbol{v}$. The exit angle θ keeps the same sign as α, while the Glory angle is not reached (Samengo and Barrachina 1994), namely for $\alpha < \arccos(v_\infty/v)$. Otherwise, it becomes negative:

$$\theta \in [0, \pi] \qquad \text{if } \alpha \leqslant \arccos(v_\infty/v)$$
$$\theta \in (-\pi, 0] \qquad \text{if } \alpha > \arccos(v_\infty/v)$$

Finally, the asymptotic relative electron–target velocity reads

$$\boldsymbol{v}_\infty = v_\infty[\cos\theta\hat{\boldsymbol{x}} + \sin\theta\hat{\boldsymbol{y}}]. \tag{4}$$

We have re-plotted the same emitted electron spectra shown in figure 3 but in terms of the new 'corrected' electron velocities (4) with respect to the target nucleus and projectile for the EEC and ECC cusps, respectively. Even though this calculation implies two distinct projections of the electron trajectories onto the Coulomb orbits around the target or projectile centres, both coincide throughout velocity space except in the close vicinity of $\boldsymbol{v} = 0$ and $\boldsymbol{v}_\mathrm{P}$, respectively, where they change the 'holes' into diverging 'cusps'. When plotted in this way, all the curves, for R equal to 100, 300, 1000, 3000, 10 000, 30 000 and 100 000 au, coincide with the one depicted in figure 3 as corresponding to $R \to \infty$, and clearly show the characteristic EEC and ECC divergencies independently of the computing time. Already at $R = 60$ au no further migration between the ionization, excitation and charge transfer channels was observed within the statistic employed in our calculation, defining a limit between what we might call the collisional and asymptotic regimes. The previous result shows that if the calculation is stopped at a relatively small distance of the order of 100 au within the asymptotic zone, and the evolution of the electron in the field of the target nucleus or projectile is analytically continued by means of equation (4), the EEC and ECC cusps are neatly recovered. Furthermore, their overall shapes and asymmetries seem to be unaffected by the asymptotic interaction with the other collision partner. In conclusion, it is not necessary to let the program proceed up to an internuclear distance of the order of 10^5 au or larger to get the EEC or ECC cusps, since they can be easily recovered by means of a simple transformation in agreement with the common understanding of cusp formation, as provided by the final state interaction theory (Barrachina 1997). Let us finally mention that the diverging nature of the ECC cusp in a CTMC calculation was shown in a previous paper (Fiol *et al* 2000) as being related to the constant value reached by the recoil ion momentum distribution at its kinematic threshold.

Next, we wanted to study the role played by the focusing of the electrons in the attractive field of the projectile. It was proposed that this is an important mechanism for cusp production, and that it is mainly operable at large internuclear distances. In fact, the progressive formation of the ECC cusp in figure 3 clearly indicates a focusing of trajectories into the forward direction. However, it is important to clarify in what sense the term 'focusing' has to be understood in

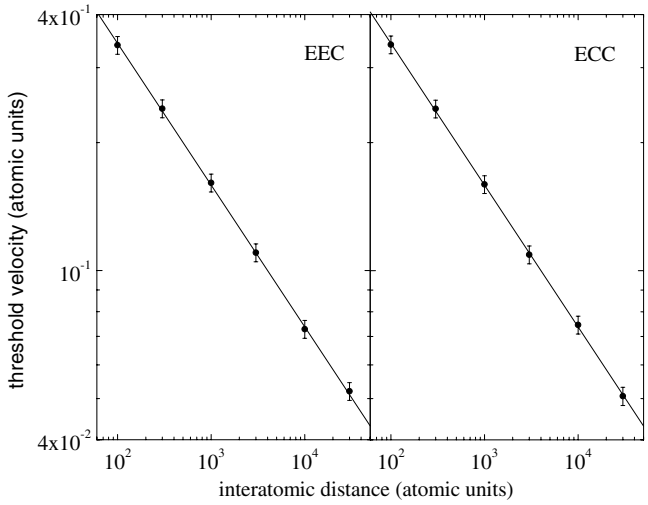

Figure 4. Velocity threshold v_h at the EEC and ECC cusps as a function of the internuclear distance R. The straight lines depict a $v_h \propto t^{-1/3}$ dependence.

the present context. By definition, a 'focusing' process would involve a perceptible deviation of the emitted electron from a straight line trajectory due to its interaction with the projectile or target nucleus. However, this is not the case when, for instance, the buildup of the ECC cusp is observed from a reference system attached to the projectile. To check this assumption, we re-plotted figure 3, but correcting only the energy and not the angle of the asymptotic electron velocity, namely

$$\boldsymbol{v}_\infty = \sqrt{1 - \frac{1/r}{m_T v^2/2}}\,\boldsymbol{v}.$$

These curves are not reproduced here, since they are again identical to the one shown in figure 3 for $R \to \infty$. This result indicates that there is no conflict between the idea of an asymptotic focusing mechanism and the final state interaction description of cusp formation as an angle independent (i.e. s-wave) process. In fact, even for not-so-large values of R, the electrons that build up the cusps are escaping from the target nucleus or the projectile in an approximately straight trajectory. In figure 4 we show a double log graph of the velocity threshold v_h that separates the continuum from bound electrons at the EEC and ECC cusps as a function of the internuclear distance R. It is readily observed that these two quantities are related by a law, $v_h \propto t^{-1/3}$. This simple result is easily obtained within a 'free expansion' model (Illescas and Riera 1998, Sidky *et al* 2000, Illescas *et al* 2002) by replacing $r \approx v_h t$ in the equation for the velocity threshold, $m v_h^2/2 = 1/r$.

4. Conclusions

In this paper we have employed the CTMC method to study the role played by the target and the projectile on the formation of the EEC and ECC cusps in ion–atom collisions. Using a variance reduction technique, we have shown that the CTMC description of cusp production is in complete accordance with the general framework of any quantum mechanical model. One important attribute of this description is that it decouples the actual ionization process from the cusp production itself. Actually, the overall shape of the cusp seems to be decided during the

collision stage, while its divergence builds up asymptotically, but mainly as the result of a two-body process. Thus, it is not necessary to let the program proceed up to very large internuclear distances to get the EEC or ECC cusps, since they can be neatly recovered by projecting the electron trajectories onto two-body continuum orbits. Finally, we showed that the presence of an asymptotic focusing mechanism does not contradict the final-state interaction description of cusp formation.

Acknowledgment

This work has been supported by the Agencia Nacional de Promoción Científica y Tecnológica (Contrato de Préstamo BID 1201/OC-AR, grant no 03-04021).

References

Abrines R and Percival I C 1966 *Proc. Phys. Soc. London* **88** 861, 873
Báder A, Sarkadi L, Vikor, Kuzel M, Závodszky P A, Jalowy T, Groeneveld K O, Macri P A and Barrachina R O 1997 *Phys. Rev.* A **55** 14
Bandarage G and Parson R 1990 *Phys. Rev.* A **41** 5878
Barrachina R O 1990 *J. Phys. B: At. Mol. Opt. Phys.* **23** 2321
Barrachina R O 1997 *Nucl. Instrum. Methods* B **124** 198
Crooks C B and Rudd M E 1970 *Phys. Rev. Lett.* **25** 1599
Fiol J, Barrachina R O and Rodríguez V 2002 *J. Phys. B: At. Mol. Opt. Phys.* **35** 149–64
Fiol J, Courbin C, Rodríguez V D and Barrachina R O 2000 *J. Phys. B: At. Mol. Opt. Phys.* **33** 5343
Fiol J, Courbin C, Rodríguez V D and Barrachina R O 2001 *22nd Int. Conf. on Physics of Electronic and Atomic Collisions* (Abstract of Contributed Papers)
Hammersley J M and Handscomb D C 1964 *Monte Carlo Methods* (London: Chapman and Hall)
Illescas C, Pons B and Riera A 2002 *Phys. Rev.* A **65** 030703(R)
Illescas C, Rabadan I and Riera A 1998 *Phys. Rev.* A **57** 1809
Illescas C and Riera A 1998a *Phys. Rev. Lett.* **80** 3029
Illescas C and Riera A 1998b *Phys. Rev. Lett.* **81** 3627
Kövér Á, Sarkadi L, Pálinkás J, Berényi D, Szabó Gy, Vajani T, Heil O, Groenenveld K O, Gibbons J and Sellin I A 1989 *J. Phys. B: At. Mol. Opt. Phys.* **22** 1595
Lewartowski E and Courbin C 1992 *J. Phys. B: At. Mol. Opt. Phys.* **25** L63
Macek J 1970 *Phys. Rev.* A **1** 235
Meckbach W, Nemirovsky I and Garibotti C 1981 *Phys. Rev.* A **24** 1793
Olson R E and Salop A 1977 *Phys. Rev.* A **16** 531
Ovchinnikov S Yu and Khrebtukov D B 1987 *15th Int. Conf. on Physics of Electronic and Atomic Collisions* (Amsterdam: North-Holland) (Abstract of Contributed Papers)
Reinhold C O, Burgdörfer J, Kemmler J and Koschar P 1992 *Phys. Rev.* A **45** R2655
Reinhold C O and Olson R E 1989 *Phys. Rev.* A **39** 3861
Rubinstein R Y 1981 *Simulation and The Monte Carlo Method* (New York: Wiley)
Rudd M E and Macek J 1972 *Case Stud. At. Phys.* **3** 48
Samengo I and Barrachina R O 1994 *Eur. J. Phys.* **15** 300
Sarkadi L, Tökési K and Barrachina R O 2000 *J. Phys. B: At. Mol. Opt. Phys.* **33** 847
Schultz D R, Reinhold C O and Olson R E 1996 *Two-Center Effects in Ion–Atom Collisions* ed T J Gay and A F Starace *(AIP Conf. Proc. vol 362)* (New York: AIP)
Sidky E Y, Illescas C and Lin C D 2000 *Phys. Rev. Lett.* **85** 1634
Tökési K, Sarkadi L and Mukoyama T 1997 *J. Phys. B: At. Mol. Opt. Phys.* **30** L123
Tökési K, Wang J and Olson R E 1994 *Nucl. Instrum. Methods* B **86** 147